



ELSEVIER

Contents lists available at ScienceDirect

Optics Communications

journal homepage: www.elsevier.com/locate/optcom

Systematic error analysis and correction in quadriwave lateral shearing interferometer



Wenhua Zhu^a, Jinpeng Li^b, Lei Chen^{a,*}, Donghui Zheng^a, Ying Yang^a, Zhigang Han^c

^a School of Electronic and Optical Engineering, Nanjing University of Science and Technology, Nanjing 210094, China

^b Nanjing Astronomical Instruments Company Limited, Chinese Academy of Sciences, Nanjing 210042, China

^c Key Laboratory of Advanced Solid-State Laser Technology, Nanjing University of Science and Technology, Nanjing 210094, China

ARTICLE INFO

Article history:

Received 10 March 2016

Received in revised form

31 May 2016

Accepted 1 June 2016

Keywords:

Error analysis

Shearing interferometry

Wavefront measurement

Diffraction gratings

ABSTRACT

To obtain high-precision and high-resolution measurement of dynamic wavefront, the systematic error of the quadriwave lateral shearing interferometer (QWLSI) is analyzed and corrected. The interferometer combines a chessboard grating with an order selection mask to select four replicas of the wavefront under test. A collimating lens is introduced to collimate the replicas, which not only eliminates the coma induced by the shear between each two replicas, but also avoids the astigmatism and defocus caused by CCD tilt. Besides, this configuration permits the shear amount to vary from zero, which benefits calibrating the systematic errors. A practical transmitted wavefront was measured by the QWLSI with different shear amounts. The systematic errors of reconstructed wavefronts are well suppressed. The standard deviation of root mean square is 0.8 nm, which verifies the stability and reliability of QWLSI for dynamic wavefront measurement.

© 2016 Elsevier B.V. All rights reserved.

1. Introduction

The wavefront of light beam will be distorted by different factors, such as air disturbance and variation of temperature, during the propagation process. Therefore, there has recently been an increasing interest in dynamic wavefront measurement, especially in astronomical optics and high-power laser fields [1,2].

The commonly used methods at present for wavefront measurement are Hartmann wavefront sensors and interferometry. The Hartmann wavefront sensors usually have a large dynamic range, but the resolution is relatively less than that of interferometry [3]. Currently the interferometric methods available for transient wavefront detection include point diffraction interferometry (PDI) and shearing interferometry (SI). PDI is a simple and self-referencing configuration to measure the wavefront quality of low temporal coherence optical beams [4]. In order to apply PDI to dynamic wavefront measurement, many novel PDIs based on synchronous phase-shifting theory have been proposed [5–7]. Besides, Zhu et al. presented a single-shot reflective shearing point diffraction interferometer (S-SRSPDI) for large-aperture wavefront measurement, which is based on Fourier transform (FT) [8–10] method [11]. However, all the proposed PDIs have a

common drawback that they are very sensitive to vibrations because the convergent beam incident on the pinhole must be stable. But for SI, it has remarkable performance in vibration environment as there is no need to introduce the absolute reference flat due to the self-reference characteristics [12]. Among shearing interferometers, multilateral shearing interferometers (multi-LSIs) are compact and stable. Moreover, thanks to the common-path configuration, multi-LSIs can be applied to the transient wavefront measurement [13]. Commonly used multi-LSIs include cross-grating lateral shearing interferometer (CGLSI) [14,15], three wave lateral shearing interferometer (TWLSI) [16] and quadriwave lateral shearing interferometer (QWLSI) based on the modified Hartmann mask (MHM) [17]. The CGLSI use a cross-grating and an order selection mask to select the ± 1 orders for lateral shearing interference. However, in order to suppress the systematic error, the cross-grating needs to be as close as possible to the order selection mask, which makes it difficult to adjust the position of each component. The QWLSI is based on the phase grating, and different types of errors may be introduced during the fabricating process of the phase grating [18]. Besides, the coma is induced in the spherical wavefront measurement. The MHM adds a specific phase chessboard to the classical Hartmann mask, and then the even orders and the multiples of 3 orders are eliminated. The diffraction efficiency of the ± 1 orders is better, but the ± 5 and ± 7 orders also remain in the diffractions. Thus the wavefront will be measured in the approach regarding the MHM as a Hartmann sensor only at the Talbot distance [19]. And the resolution is also

* Corresponding author.

E-mail addresses: mlwdjq@njjust.edu.cn (W. Zhu), chenlei@njjust.edu.cn (L. Chen).

limited compared to conventional interferometers. The TWLSI uses an afocal system to suppress all the parasitic orders. In this configuration, the resolution of detector can be more effectively used, but the systematic errors introduced by the afocal system limit the accuracy of the TWLSI.

In this paper, the systematic error of the QWLSI is analyzed and corrected to obtain high-precision and high-resolution measurement of dynamic wavefront. The configuration of the QWLSI is similar to the TWLSI. Specially, we introduce a collimating-lens to collimate the spherical wavefronts, which are diffracted by chessboard grating and filtered by order selection mask, to eliminate the errors caused by the shear of spherical wavefronts and the tilt of CCD target. Besides, this configuration permits the shear amount to vary from zero, which can be used to calibrate the systematic errors. With the systematic error corrected, the interferometer can be used for dynamic wavefront measurement, especially for large-aperture.

2. Theory

The scheme of the QWLSI is depicted in Fig. 1. The convergent wavefront under test is diffracted by a chessboard grating to produce multiple replicas. And then by a square order selection mask lied in the focal plane of the replicas, the $(\pm 1, \pm 1)$ orders are selected. After that, the selected orders are collimated by a collimating lens before interfering with each other to form a lateral shearing interferogram at the CCD target.

According to the symmetry, we only give the optical paths of the $(\pm 1, 1)$ diffraction orders. O_1 is conjugated with the focus O_1 of the $(1, 1)$ diffraction order while O_2 with the focus O_2 of the $(-1, 1)$ diffraction order. Set the origin of coordinates at the center of collimating lens. The aberrations included in the wavefront under test is denoted as $W_A(x, y)$. W_{pq} , where $p, q = \pm 1$, are defined as the total aberrations caused by the chessboard grating and collimating lens in four replicas respectively. Then the complex amplitude of the $(\pm 1, \pm 1)$ diffraction orders at CCD target can be expressed as

$$U_{pq}(x, y) = \frac{tA}{z - l_2} \exp \left\{ ik \left[r(x - pd_2, y - qd_2) + W_{pq} \right] \right. \\ \left. + W_A(x - ps/2, y - qs/2) \right\}, \quad (1)$$

where t is the $(\pm 1, \pm 1)$ diffraction efficiency of the chessboard grating, A is the amplitude of the incident wavefront, z is the distance from the principal plane of collimating lens to CCD target while l_3 is the distance from the one to O_1 or O_2 , $k = 2\pi/\lambda$ is the wavenumber, λ is the wavelength of incident wavefront, d_2 is distance between O_1 and O_2 , s is the shear amount. $r(x, y)$ is the curvature radius of the spherical wavefront, which can be expressed as

$$r(x, y) = z - l_3 - \frac{x^2 + y^2}{2(z - l_3)} + \frac{(x^2 + y^2)^2}{8(z - l_3)^3} \quad (2)$$

according to Taylor series expansion. Thus combining Eq. (1) with (2), the intensity distribution of the interferogram at the CCD target, which is produced by superimposing the $(\pm 1, \pm 1)$ diffraction orders, can be written as

$$I(x, y) = \left[\sum_{p,q=\pm 1} U_{pq}(x, y) \right] \left[\sum_{p,q=\pm 1} U_{pq}^*(x, y) \right] \\ = I_0 \left(\cos \left\{ k \left[\frac{d_2 \partial r(x, y - \frac{d_2}{2}) + s \partial W_A(x, y - \frac{s}{2})}{\partial x} + W_{11} - W_{-11} \right] \right\} + \right. \\ \left. \cos \left\{ k \left[\frac{d_2 \partial r(x, y + \frac{d_2}{2}) + s \partial W_A(x, y + \frac{s}{2})}{\partial x} + W_{1-1} - W_{-1-1} \right] \right\} + \right. \\ \left. \cos \left\{ k \left[\frac{d_2 \partial r(x - \frac{d_2}{2}, y) + s \partial W_A(x - \frac{s}{2}, y)}{\partial y} + W_{11} - W_{1-1} \right] \right\} + \right. \\ \left. \cos \left\{ k \left[\frac{d_2 \partial r(x + \frac{d_2}{2}, y) + s \partial W_A(x + \frac{s}{2}, y)}{\partial y} + W_{-11} - W_{-1-1} \right] \right\} \right. \\ \left. + \cos \left\{ k \left[\frac{d_2 \partial r(x, y) + s \partial W_A(x, y)}{\partial(x+y)} + W_{11} - W_{-1-1} \right] \right\} + \right. \\ \left. \cos \left\{ k \left[\frac{d_2 \partial r(x, y) + s \partial W_A(x, y)}{\partial(x-y)} + W_{1-1} - W_{-11} \right] \right\} + 2 \right) \quad (3)$$

where

$$\begin{cases} \frac{\partial r(x, y)}{\partial x} = -\frac{x}{z - l_3} + \frac{x(x^2 + y^2)}{2(z - l_3)^3} \\ \frac{\partial r(x, y)}{\partial y} = -\frac{y}{z - l_3} + \frac{y(x^2 + y^2)}{2(z - l_3)^3} \\ \frac{\partial}{\partial(x \pm y)} = \frac{\partial}{\partial x} \pm \frac{\partial}{\partial y} \end{cases} \quad (4)$$

$I_0 = 2t^2A^2/(z - l_3)^2$. Eq. (4) gives the difference expression of two spherical wavefronts. According to aberration theory [20], the difference of two spherical wavefronts introduces not only a high linear-carrier frequency but also a coma. Besides, it can be seen from Eq. (3) that both the manufacturing error of chessboard grating and the transmitted distortion of collimating lens are introduced into the difference wavefronts in all directions. Therefore, we will discuss how to eliminate these errors to reconstruct the wavefront under test with high accuracy. On the other hand, in Eq. (3), we can find both the difference wavefronts in x and y directions contain two cosine functions which are not exactly equal in the case of ignoring systematic errors. However, due to the symmetry, the carrier frequency of the two cosine functions are

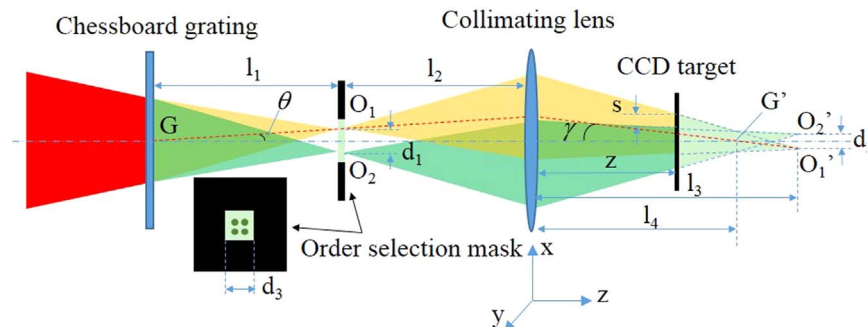


Fig. 1. Schematic diagram for the $(\pm 1, 1)$ diffraction orders shearing.

Download English Version:

<https://daneshyari.com/en/article/1533038>

Download Persian Version:

<https://daneshyari.com/article/1533038>

[Daneshyari.com](https://daneshyari.com)